ISSN: 0975-3583, 0976-2833 VOL 12, ISSUE 03, 2021

# Identification Of Serum Metabolites As Early Predictors Of Doxorubicin Induced Cardiac Hypertrophy

**[1]Dharaniyambigai Kuberapandian,, [2]* Dr. Victor Arokia Doss**
**Department of Biochemistry, PSG College of Arts & Science,**
**Coimbatore, Tamil Nadu, India.**
[1]Research Scholar, Department of Biochemistry,PSG College of Arts & Science,Coimbatore, Tamil Nadu, India.E-mail: dharaniyambigai.kuberan@gmail.com Orcid: 0000-0003-3958-7868
[2]Associate Professor,Department of Biochemistry,PSG College of Arts & Science,Coimbatore, Tamil Nadu, India.E-mail: victordoss64@gmail.comOrcid: 0000-0002-4326-6840
**Corresponding Author: Dr. Victor Arokia Doss**

**ABSTRACT**
**Background:** Cardiac hypertrophy (CH) is the asymptomatic enlargement of cardiac ventricles induced during doxorubicin (DOX) administration and the lack of its early detection imposes survival risk.
**Objectives:** This study on the seven diagnostic parameters of CH comorbidities, QRS complex, R-amplitude, R-R interval and heart rate (HR) of ECG, 3-hydroxybutyrate (3-HB), lactic acid (LA), urea as the responders of metabolic shifts in DOX induced CH for which the early identification of serum predictors and their putatively affected pathways were attempted.
**Methods:** Male Sprague Dawley rats (n=5) were administered DOX (2.5 mg/kg, i.p, 2 weeks, every 5$^{th}$ day). Cardiotoxicity was evaluated using electrocardiography (ECG), heart weight (HW)/body weight (BW) ratio and histopathological analysis. Gas chromatography mass spectrometry (GC-MS) analysis was performed to screen the serum metabolites. Pearson's correlation followed by multiple regression analysis (MRA) identified strongly significant predictor metabolites. Significantly affected pathways were identified using Metabolite set enrichment analysis (MSEA). All the data were verified statistically ($P<0.05$).
**Results:** DOX administered rats exhibited CH commencement whose serum metabolite analysis using GC-MS, correlation, MRA identified sorbitol as the significant early predictor for R-amplitude, isoleucine for R-R interval, mannonic acid for HR, cholesterol for 3-HB, succinic acid for LA and urea. No significant relationship or predictor were identified for QRS complex. MSEA mapped branched chain amino acid (BCAA) degradation and ketone body metabolism as the highly impactable significant pathways by the significant 5 predictors.
**Conclusion:** This study identified significant predictors and pathways that can aid in early detection and intervention of CH induced by DOX.
**Key words:** Doxorubicin, cardiac hypertrophy, early predictors, GC-MS, correlation, regression.

## 1. INTRODUCTION

Cardiac hypertrophy (CH) is a clinical condition in which the cardiac ventricles, preferably the left ventricle becomes enlarged due to the impaired architecture of extracellular matrix proteins, especially collagen whose accumulation is termed as cardiac fibrosis (CF). This result due to the metabolic shifts that arise initially to combat the cellular stress and compensate the energy metabolism in order to maintain the physiological cardiac events. Due course, the shift in preferences for metabolite substrates (example fatty acid to glucose) and metabolic pathways occur which is termed as metabolic reprogramming or remodelling and during chronic states it gradually develops into the asymptomatic CH [1-3]. CH is prevalent not only among patients with prevailing clinical histories like diabetes, hypertension, obesity, chronic kidney disease (CKD) but is also witnessed in paediatric and adult cancer patients [4-6]. The administration of anticancer drugs, the anthracyclines especially doxorubicin (DOX) to cancer patients has not only been well-reported for its therapeutic potential but also for its deleterious cardiotoxicity [7]. DOX induced cardiotoxicity are screened as the asymptomatic and irreversible CH that presents itself only after significant cardiac injury during 2D-echocardiographic analysis [8]. Wide reports are available on the pathophysiology of DOX induced CH on the basis of oxidative stress and apoptotic mechanisms due to aberrant nuclear factor-erythroid-derived 2-related factor 2 (Nrf2) associated antioxidant systems that trigger mechanisms that produce advanced glycated end products (AGEs) favouring CF which were identified as therapeutic targets [9-12]. Treatments for DOX induced cardiotoxicity include antioxidant supplements, angiotensin converting enzyme (ACE) inhibitors, α-adrenergic receptor agonists, cell therapy using differentiated embryonic stem cells

ISSN: 0975-3583, 0976-2833 VOL 12, ISSUE 03, 2021

(ESCs) and inducible pluripotent stem cells (iPSCs) [6]. Recently, early detection using nuclear magnetic resonance (NMR), hyperpolarized magnetic resonance imaging (MRI) of the heart tissues coupled with blood analysis using liquid chromatography mass-spectrometry (LC-MS) were attempted to identify low levels of cardiac injury by DOX at initial stage. In all these previous studies the focus on understanding the shifts between metabolites that can be easily detectable in serum and their relationship that aid in early prediction for DOX induced cardiotoxicity are less explored [6,8,13].

3-hydroxybutyrate (3-HB), lactic acid (LA), urea [14-16] and ECG parameters namely QRS complex, R-amplitude, R-R interval and heart rate (HR) were widely reported and diagnosed in various CH comorbidities like diabetes, obesity, hypertension and CKD [17-19]. The current study proposed that these seven factors can be assumed as the responders of CH due to the consequences of metabolic remodeling which is influenced by various shifts in metabolite levels. Therefore, these seven factors were considered as the dependent variables whereas the metabolite that influences it as the independent variable in this study. Hence, the present study attempted to screen the changes in these seven responders, identify their metabolite predictors in serum and the putative pathways affected during DOX induced early CH using metabolomic statistical programmes correlation, multiple regression analyses (MRA) and metabolite set enrichment analysis (MSEA).

## 2. MATERIALS AND METHODS

### 2.1. Chemicals

All chemicals and reagents used were analytical grade from Hi Media Pvt Ltd., India. *N*-Trimethylsilyl-*N*-methyl trifluoroacetamide (MSTFA), Methoxyamine hydrochloride were purchased from Sigma-Aldrich, doxorubicin (10mg/5ml injection vials) were purchased ethically from the licensed pharmacy shop at Coimbatore.

### 2.2. Experimental groups

Male Sprague Dawley rats weighing between 100 to 110 g were procured after ethical clearance (CPCSEA/No:399/2018/IAEC) and acclimatized for 3 days under controlled temperature (29°C ± 5°C), humidity (55% ± 5%), and 12 hours of light/dark cycles. They were divided into two groups (n = 5 rats each):-

Group 1 – normal (control - NOR);

Group 2 - doxorubicin (DOX) (2.5 mg/kg, i.p, 2 weeks, every 5$^{th}$ day) [20]

The normal group in this study was also used for our previous similar concomitant study conducted in our lab.

### 2.3. Electrocardiography (ECG) analysis

The development of CH was screened with ECG conventional bipolar limb lead II using BITalino ECG Sensor - OpenSignals [r]evolution software for six minutes in unanaesthetised rats to record the changes in QRS complex, R amplitude, R–R interval and pulse/heart beat rate (HR). Their percentage changes were calculated as [(ECG parameter value in DOX - in NOR) / (in NOR) x100] [21,22].

### 2.4. Hypertrophic index (HW/BW ratio)

The hypertrophic index was determined using the heart weight (HW)/ body weight (BW) ratio among experimental groups [21].

### 2.5. Histopathological analysis of left and right ventricles

The excised heart tissues were excised, processed and stained with haematoxylin and eosin (H&E) stain to examine their cellular architecture of the left and right ventricles at 40X [23].

### 2.6. Gas Chromatography-Mass Spectroscopy (GC-MS) analysis of serum metabolites

Serum was isolated from the blood (cardiac-puncture post over-night fasting) and derivatized as per the modified protocol [24]. Briefly, precipitation of 100 µl serum was done using 250 µl acetonitrile and evaporated to dryness using $N_2$ gas. 20 mg methoxylamine hydrochloride dissolved in 1 ml pyridine was added, incubated at 70°C for 60 minutes to which 50 µl MSTFA was added and incubated 40 °C for 90 minutes. 1 µl of thus derivatized sample was injected into the inlet port at 10:1 split mode. GC-MS analysis was done using Shimadzu GC-2010 plus gas chromatography instrument coupled to a Shimadzu QP2010 mass spectrometer (Shimadzu, Japan). Helium served as carrier gas set at a flow rate of 1 ml/minute with the initial temperature as 100°C for 4 minutes which was raised to 270°C at the rate of 5°C/minute. The temperatures of injection was set at 280°C, interface at 250°C and ion source at 200°C with a solvent delay of 9 minutes. MS was operated in electron ionisation mode (70 eV; m/z of 35 to 800) followed by the identification of metabolites based on NIST & WILEY mass library (ribitol as reference).

### 2.7. Data analysis

ISSN: 0975-3583, 0976-2833 VOL 12, ISSUE 03, 2021

Specific and comprehensive analysis using Pearson's correlation along with pattern search analysis and metabolite set enrichment analysis (MSEA using SMPDB library) were done with MetaboAnalyst 4.0. Multiple regression analysis (MRA) and individual linear regression prediction models were performed using IBM SPSS 26.0 that verified data (expressed as mean ± standard error of the mean) statistically using ANOVA with significance at $P < 0.05$ [25,26].

## 3. RESULTS

### 3.1. ECG screening for CH in DC

DOX administered rats exhibited significantly elevated R-amplitude with prolonged R-R interval and declined heart beat rate (HR) though the QRS complex did not show significant widening as shown in table 1 and figure 1.

### 3.2 Hypertrophic index (HW/BW ratio)

The HW and HW/BW ratio were significantly increased in DOX administered rats whereas no significant difference was observed in BW as shown in table 2. The heart size was noticeably enlarged in DOX administered rats when compared to normal as shown in figure 2.

### 3.3. Histopathological analysis

The H&E staining of left and right ventricles exhibited cellular derangement with striations, hypertrophied nuclei and infiltrations in the DOX administered rats as depicted in figure 3.

### 3.4. Metabolite profiling and shifts using GC-MS analysis.

Figure 4 shows the concentration of serum metabolites namely amino acids, sugars, lipids, 3-hydroxybutyrate (3-HB), lactic acid (LA) and urea among which all the metabolites except alanine, galactose and mannose were found to be elevated in the DOX administered rats.

### 3.5. Correlation analysis between metabolites (independent factors) and diagnostic parameters (dependent factors)

Pearson's correlation-based pattern hunting analysis revealed the relationship between the positively and negatively correlated serum metabolites that were screened using GC-MS. It also depicted the strongly related metabolites (Pearson's score > 0.7) between themselves and as well as with the diagnostic parameters, herein the metabolic responders of remodeling (3-HB; LA; urea; ECG waves namely QRS complex, R-amplitude, R-R interval and heart rate) as shown in figures 4 and 5. Unlike other metabolites, alanine, galactose and mannose were the only positively correlating metabolites with HR and between themselves but negative with others among which galactose was found as the most strongly associated metabolite with the responders as shown in figures 5 and 6.

### 3.6. Serum predictors for the metabolic responders using MRA

MRA indicated the most significant and influential predictor metabolites for each of the seven diagnostic parameters, herein the metabolic responders as shown in table 3. It also shows the linear equation for each predictor along with the fit values indicated by P and $R^2$ values which were highly significant ($P < 0.05$) and $R^2$ scores were greater than 0.9.

### 3.7. Pathways influenced by significant predictors

MSEA revealed that branched-chain amino acids (BCAA – valine, leucine, isoleucine) degradation and ketone body metabolisms were identified as the significant ($P < 0.05$) and apparent pathways that can be highly influenced by the five significant predictors in DOX administered rats as shown in figure 7. The figure also shows the list of other less significant ($P > 0.05$) pathways that could be impacted by the significant predictors.

## 4. DISCUSSION

DOX cardiotoxicity has been previously explored through genetic and protein expression studies associated with apoptosis, fibrosis, cell growth, hypertrophy and inflammation [7,27,28]. Previous studies reported the changes in ECG beyond 7 days of DOX administration based on the acute cardiotoxicity investigated for 2 weeks and chronically for 6 weeks durations but the focus on metabolic perspectives behind these changes were minimal [19,29,30]. Till date no specific treatment for total recovery caused by DOX is available due to the lack of understanding on the exact metabolic mechanisms and early events involved in the development of CH thereby making the prediction and prevention of adverse CH difficult. Combination of metabolomic analysis and bioinformatics have been previously represented as a promising tools for better understanding of acute DOX cardiotoxicity in cardiac tissue though the heart did not show any significant abnormalities [20,13].

Recently, an investigation attempted to integrate precision medicine with artificial intelligence wherein the ECG data were used to train datasets that enabled the prediction of blood glucose without any blood retrieval [31]. In a similar approach, the present study attempted to understand the early cardiac physiology, serum metabolites and their relationships by integrating the data from electrocardiography (ECG), GC-MS with the statistical approaches, correlation and MRA respectively.

ISSN: 0975-3583, 0976-2833 VOL 12, ISSUE 03, 2021

This study identified significant predictor metabolites for the seven factors that respond during metabolic modulations of CH namely QRS complex, R amplitude, R-R interval, HR, 3-HB, LA and urea. This study was also extended to identify metabolic pathways in which the identified predictors were reported to participate and might be putatively involved during early metabolic alterations.

Widened QRS complex, elevated R-amplitude, prolonged R-R interval, reduced HR, increased HW, HW/BW ratio accompanied by impaired myocardial organization are the primary characteristics of CH [21,17,32]. This study also exhibited similar characteristics that hereby confirm the existence of CH, except the insignificant QRS complex that illustrated no prompt changes in ventricular depolarization. This was coherent with the correlation results that showed no significantly related metabolites for QRS complex and hence no predictors were identified based on relationship. However, in previous studies widened QRS complex and its amplitude were observed only at either higher DOX dosage (15mg/kg body weight) or during extended duration beyond 2 weeks [19,30]. This strengthens our findings that the observation recorded here were only the consequences of early initiation of CH at the end of 2 weeks with the commencement of dysfunction in ventricular depolarization through cumulative dosage of 10mg/kg DOX. The values of normal group indicated in this study were also used in a similar study conducted in our lab along with this study concomitantly [33] wherein we identified serum predictors for isoproterenol and N-acetyl-L-cysteine (NAC) induced cardiac hypertrophic rat models. Though the present study did not provide predictor metabolites for QRS complex to aid in early prediction, this study recommends the significant predictors identified for other responders of ventricular depolarization such as R-amplitude, R-R interval and ultimately HR [22].

Elevated sorbitol levels identified in DOX administered rats were identified as the significant predictor for R-amplitude. Sorbitol is a well-known metabolite of the polyol pathway, an alternate glucose utilization route besides glycolysis by the action of aldose reductase which is predominant in the hypertrophied heart [33]. Accumulation of sorbitol has been previously reported with elevated oxidative stress, reduced $Na^+/K^+$ ATPase, inadequate ATP, stimulation of AGEs that enhance fibrotic events though the mechanisms underlying them are still unclear [34]. So far only meagre reports are available on the metabolic consequences of sorbitol accumulation and its degradation that affects HR by the activation of sorbitol dehydrogenase, an enzyme that converts sorbitol into fructose [35]. This present study is the first to report the crucial role of sorbitol and its mechanisms as a putative influencer and predictor of R-amplitude during the initiation of CH induced by DOX.

R-R interval that indicates the duration between successive beats [22] whose predictor have been identified in this study as isoleucine, a branched-chain amino acid (BCAA). In addition, BCAA degradation pathway was also coherently mapped as one of the highly influential metabolic pathway during early DOX cardiotoxicity in this study. Previously, defects in catabolism of BCAA have been reported as a crucial pathophysiology underlying heart failure wherein isoleucine was shown to have effect upon fatty acid oxidation through peroxisome proliferator activator receptor α (PPARα) [36]. Similar to this study, we observed isoleucine as the significant predictor of cardiac rhythm in isoproterenol induced CH [33]. Studies indicate that such elevated isoleucine and BCAAs were previously observed during cardiac injuries in high salt diet rat models [37] similar to this study probably due to the impaired catabolic events. Such events induce mitochondrial impairment, cellular stress and cardiac dysfunction [38] which justifies isoleucine as a potent predictor among the 3 BCAA during the early DOX effects.

This is the first study to our knowledge that reported mannonic acid as a predictor for HR. As mannonic acid has not been previously associated with any *in vivo* system models like humans or rats, this study hypothesizes the possible interconversion reaction between gluconic acid and mannonic acid that occurs during heating with pyridine [39] which was performed during derivatization protocols for GC-MS analysis. So, though GC-MS analysis identified the metabolite as mannonic acid, this study hypothesizes D-gluconic acid as the hidden predictor metabolite present *in vivo* as it has been previously well-reported to be linked with the sorbitol pathway and mechanisms linked with energy production [40].

3-HB has been reported previously as a metabolic stress defence metabolite that elevates due to cellular adaptative mechanisms [14]. Enormous studies reported the therapeutic potential of 3-HB and the other ketone bodies, acetoacetate and acetone in treating hypoxia and heart failure [41]. The present study identified elevated cholesterol as the significant predictor of elevated serum levels of 3-HB. It has already been well established that the oxidation of circulating ketone bodies is involved in the biosynthesis of cholesterol [42]. A recent investigation by us [33] also has showcased low levels of cholesterol influencing cardiac rhythm in isoproterenol administered rats during CH. This strengthens our findings that cholesterol levels can be used to predict 3-HB whose levels can in turn be used to

ISSN: 0975-3583, 0976-2833 VOL 12, ISSUE 03, 2021

track the on-set of CH induced by DOX. To add, as the five predictors identified in this study are well - known to be associated directly and indirectly with acetyl coenzyme A, the key source for ketone body synthesis and oxidation [43], any alteration in the levels of predictor metabolites can influence ketone body metabolism as identified by the MSEA in this study.

Succinic acid has been previously reported as a crucial metabolite in the pathophysiology of CH. Elevated serum succinate levels chronically increases blood pressure. Succinate has been reported to be linked with processes underlying ischemia and in CH associated with obstructive coronary artery diseases [44]. During such condition oxygen deprivation termed as hypoxia might occur and it has been reported previously that lactate levels increase during hypoxia and CH [45]. In our recent findings [33] we identified succinic acid as a potent predictor that influences cardiac rhythm in isoproterenol and NAC administered hypertrophic rats. Previous researches reported that the levels of succinate and lactate were concomitantly impaired and elevated in the process of restoring energy equivalents like $NAD^+$ during cardiac overload [46]. These advocate the predictor-responder relationship between succinate and lactic acid identified in this study.

Elevated succinic acid was also identified as the predictor for increased serum urea in this study. No direct relationship between succinic acid and urea have been reported previously except for a study which listed few metabolites commonly shared by them like malonyl coenzyme A, propionyl coenzyme A that effect the urea synthesis [47]. Exceptionally, a study had shown that administration of succinic acid increases urea levels during hepatic and kidney injuries. Hence, besides succinic acid being a key stabilizer of ion metabolism by regulating mitochondrial events [48,49], the identification of succinate as a potent putative predictor by this study hereby warrants further understanding with its responders, LA and urea.

Thus, an integration between metabolism and statistical machine-learning algorithms aided in understanding early metabolite shifts and relationship between serum metabolites based on which the potent putative early serum predictors namely sorbitol, isoleucine, mannonic or gluconic acid, cholesterol and succinic acid were identified. Also, the BCAA degradation and ketone metabolism were depicted as the apparently affected metabolic pathways during the acute or early DOX induced CH. This study recommends such an integrative approach on larger samples so that it can provide insights on early events of DOX cardiotoxicity. Its application can ultimately enhance the prediction, treatment and survival opportunities in cardiac hypertrophy.

**Acknowledgement**

We hereby acknowledge Department of Science and Technology (DST), Government of India for the Proposal Grant (SR/WOS-A/LS-480/2018) to perform this fundamental study which is a part of the proposal. We thank CPCSEA, India and PSG Institutional Animal Ethics Committee, PSGIMS & R, Coimbatore for providing animal ethical clearance. We thank Rattan labs, Coimbatore for supporting the histopathological analysis. We also thank PSG College of Arts & Science for providing the infrastructure and necessary administrative support.

**Conflict of Interests**

None.

**References**

1. Gibb AA, Hill BG. Metabolic coordination of physiological and pathological cardiac remodelling. Circ Res. 2018; 123: 107-128.

2. Mosqueira D, Smith JGW, Bhagwan JR, Denning C. Modeling hypertrophic cardiomyopathy mechanistic insights and pharmacological intervention. Trends Mol Med. 2019; 25 (9): 775-790.

3. Frey N, Katus HA, Olson EN, Hill JA. Hypertrophy of the Heart. A new therapeutic target. Circulation. 2004; 109: 1580-1589.

4. Finnocchiaro G, Magavem E, Sinagra G, Ashley E, Papadakis M, Eateban MT, et al. Impact of demographic features, lifestyle and comorbidities on the clinical expression of hypertoprhic cardiomyopathy. J Am Heart Assoc. 2017;6: e007161.

5. Molina MS, Penalver MN, Esparza CM, Esteban-Gil A, Santos-Maleo JJ, Gimeno JR. Genetic factors involved in cardiomyopathies and in cancer. J Clin Med. 2020; 9, 1702:1-26.

6. Santos DS, Goldenberg RCS. Doxorubicin-induced cardiotoxicity: From mechanisms to development of efficient therapy. In: Tan W, editor. Cardiotoxicity. Intechopen; 2018. 1-22.

7. Octavia Y, Tocchetti CG, Gabrielson KL, Janssens S, Crijns HJ, Moens AL. Doxorubicin-induced cardiomyopathy: From molecular mechanisms to therapeutic strategies. **J** Mol Cell Cardiol. 2012. 52: 1213-1225.

8. Madonna R. Early diagnosis and prediction of anticancer drug-induced cardiotoxicity: from cardiac imaging to “Omics” technologies. Rev Esp Cardiol (Engl Ed). 2017. 70 (7): 576-582.

ISSN: 0975-3583, 0976-2833 VOL 12, ISSUE 03, 2021

9. Li S, Wang W, Niu T, Wang H, Li B, Shao L, et al. Nrf2 deficiency exaggerates doxorubicin-induced cardiotoxicity and cardiac dysfunction. Oxid Med Cell Longev. 2014. 2014 (748524): 1-15.
10. Guo Z, Yan M, Chen L, Fang P, Li Z, Wan Z, et al. Nrf2-dependent antioxidant response mediated the protective effect of tanshinone IIA on doxorubicin-induced cardiotoxicity. Exp Ther Med. 2018. 16: 3333-3344.
11. Shanmugam G, Wang D, Gounder SS, Fernandes J, Litovsky SH, Whitehead K, et al. Reductive stress causes pathological cardiac remodeling and diastolic dysfunction. Antioxid Redox Signal. 2020. 32 (18): 1-20.
12. Moriyama T, Kemi M, Okumura C, Yoshihara K, Horie T. Involvement of advanced glycation end-products, pentosidine and $N^{\varepsilon}$-(carboxymethyl)lysine in doxorubicin-induced cardiomyopathy in rats. Toxicology. 2010. 268: 89-97.
13. Rasanen M, Degerman J, Nissinen TA, Miinalainen I, Kerkela R, Siltanen A, et al. VEGF-B gene therapy inhibits doxorubicin-induced cardiotoxicity by endothelial protection. PNAS. 2016. 113 (46): 13144-13149.
14. Horton JL, Davidson MT, Kurishima C, Vega RB, Powers JC, Matsuura TR, et al. The failing heart utilizes 3-hydroxybutyrate as a metabolic stress defense. JCI Insight. 2019. 4(4): 1-19.
15. Fizel A, Fizelova A. Cardiac hypertrophy and heart failure: Dynamics of changes in high-energy phosphate compounds, glycogen and lactic acid. J Mol Cell Cardiol. 1971. 2: 187-192.
16. Siedlecki AM, Jin X, Muslin AJ. Uremic cardiac hypertrophy is reversed by rapamycin but not by lowering of blood pressure. Kidney Int. 2009. 75 (8): 800-808.
17. Sysa-Shah P, Sorensen LL, Abraham MR, Gabrielson KL. Electrographic characterization of cardiac hypertrophy in mice that overexpress the ErbB2 receptor tyrosine kinase. Comp Med. 2015. 65 (4): 295-307.
18. Dilva DVJ, Neto FE, Salgado HC, Junior FR. Chronic converting enzyme inhibition normalizes QT interval in aging rats. BJMBR. 2002. 35: 1025-1031.
19. Ahmed AZ, Satyam SM, Shetty P, D'Souza MR. Methyl gallate attenuates doxorubicin-induced cardiotoxicity in rats by suppressing oxidative stress. Scientifica. 2021. 6694340:1-12.
20. Chen Y, Tang Y, Zhang Y-C, Huang X-H, Xie Y-Q, Xiang Y. Metabolomic study of rats with doxorubicin-induced cardiomyopathy and Shengmai injection treatment. PlosOne. 2015. E0125209: 1-20.
21. Doss VA, Kuberapandian D. Evaluation of anti-hypertorphic potential of Enicostemma littorale Blume on isoproterenol induced cardiac hypertrophy. Indian J Clin Biochem. 2019. 36: 33-42.
22. Konopelski P, Ufnal M. Electrocardiography in rats: a comparison to human. Physiol Res. 2016. 65: 712-725.
23. Zahkouk SA, El-Gendy AM, Eid FA., El-tahway NA, El-Shamy SA. Physiological and histological studies on the heart of male albino rats exposed to electromagnetic field and the protective role of Silymarin and/or Vitamin E. Egypt J Hosp Med. 2015. 58: 94-108.
24. Sowndarya R, Doss VA. Identification of metabolomic changes before and after exercise regimen in stress induced rats. J Environ Biol. 2017. 38:517-522.
25. Chong J, Wishart DS, Xia J. Using Metaboanalyst 4.0 for comprehensive and integrative metabolomics data analysis. Curr Protoc Bioinformatics. 2019. 68(1):e68.
26. Dhakal CP. Interpreting the basic output (SPSS) of multiple linear regression. IJSR. 2019. 8(6):1448-1452.
27. Damiani RM, Moura DJ, Viau CM, Caceres RA, Henriques JAP, Saffi J. Pathways of cardiac toxicity: comparison between chemotherapeutic drugs doxorubicin and mitoxantrone. Arch Toxicol. 2016. 90 (9): 2063-2076.
28. Ghigo A, Li M, Hirsch E. New signal transduction paradigms in anthracycline-induced cardiotoxicity. Biochim Biophys Acta. 2016. 1863 (7 Pt B): 1916-1925.
29. Ammar ME, Said SA, Suddek GM, El-Damarawy SL. Amelioration of doxorubicin-induced cardiotoxicity by deferiprone in rats. Can J Physiol Pharmacol. 2011. 89: 269-276.
30. Wu R, Wang H-L, Yu H-L, Cui X-H, Xu M-T, Xu X, et al. Doxorubicin toxicity changes myocardial energy metabolism in rats. Chem Biol Interact. 2016. 244: 149-158.
31. Porumb M, Stranges S, Pescape A, Pecchia L. Precision medicine and artificial intelligence: A pilot study on deep learning for hypoglycemic events detection based on ECG. Sci Rep. 2020. 10 (170): 1-16.
32. Karale S, Yamuna PV, Kamath JV. Protective effect of capsaicin against doxorubicin induced cardiotoxicity in experimental rats. Indian J Pharm Educ Res. 54 (1): 95-100.
33. Kuberapandian D, Doss VA. Identification of serum predictors of n-acetyl-l-cysteine and isoproterenol induced remodelling in cardiac hypertrophy. Turk J Biol. 2021. 45: 323-332.

ISSN: 0975-3583, 0976-2833 VOL 12, ISSUE 03, 2021

34. Asbun J, Villarreal FJ. The pathogenesis of myocardial fibrosis in the setting of diabetic cardiomyopathy. J Am Coll Cardiol. 2006. 47 (4): 693-700.
35. Tran DH, Wang ZV. Glucose metabolism in cardiac hypertrophy and heart failure. J Am Heart Assoc. 2019. 8 (e012673): 1-18.
36. Mathias AO, Victor OB, Ayodele SO. Carvedilol improves sorbitol dehydrogenase and heart rate variability indices thereby ameliorating cardiac autonomic neuropathy in T1DM rats with streptozotocin-induced diabetes. Am J Biomed Sci & Res. 2020. 7(5): 434-440.
37. Huang Y, Zhou M, Sun H, Wang Y. Branched-chain amino acid metabolism in heart disease: an epiphenomenon or a real culprit. Cardiovasc Res. 2011. 90: 220-223.
38. Sun H, Olson KC, Gao C, Prosdocimo DA, Zhou M, Wang Z, et al. Catabolic defect of branched-chain amino acids promotes heart failure. Circulation. 2016. 133(21): 2038-2049.
39. Wende AR, Brahma MK, McGinnis GR, Young ME. Metabolic origins of heart failure. JACC: Basic to translational Science. 2017. 2 (3): 297-310.
40. Bonnett HT, Upson FW. The action of alkalies on the monobasic sugar acids. I. Conversion of gluconic to mannonic and of galactonic to talonic acids by the action of barium hydroxide. J Am Chem Soc. 1933. 55 (3): 1245–1248.
41. Forman DT, Wiringa K. Enzyme changes in diabetes mellitus. Ann Clin Lab Sci. 1973. 3(5): 374-385.
42. Chakraborty S, Galla S, Cheng X, Yeo J-Y, Mell B, Singh V, et al. Salt-responsive metabolite, β-hydroxybutyrate, attenuates hypertension. Cell Rep. 2018. 25 (3): 677-689.
43. Cotter DG, Schugar RC, Crawford PA. Ketone body metabolism and cardiovascular disease. Am J Physiol Heart Circ Physiol. 2013. 304 (8): H1060-H1076.
44. Puchalska P, Crawford PA. Multi-dimensional roles of ketone bodies in fuel metabolism, signaling and therapeutics. Cell Metab. 2017. 25 (2): 262-284.
45. Aguiar CJ, Rocha-Franco JA,Sousa PA, Santos AK, Ladeira M, Rocha-Resende C, et al. Cell Commun Signal. 2014. 12(78): 1-17.
46. Taegtmeyer H. Metabolic responses to cardiac hypoxia: Increased production of succinate by rabbit papillary muscles. Circ Res. 1978. 43 (5): 808-815.
47. O'Donnell, Kudej RK, LaNoue KF, Vatner SF, Lewandowski ED. Limited transfer of cytosolic NADH into mitochondria at high cardiac workload. Am J Physiol Heart Circ Physiol. 2004.286: H2237–H2242.
48. Tretter L, Patocs A, Chinopoulos C. Succinate, an intermediate in metabolism, signal transduction, ROS, hypoxia and tumorigenesis. Biochim Biophys Acta. 2016. 1857: 1086-1101.
49. Lieshchova MA, Bilan MV, Bohomaz AA, Tishkina NM, Brygadyrenko VV. Effect of succinic acid on the organism of mice and their intestinal microbiota against the background of excessive fat consumption. Regul Mech Biosyst. 2020. 11(2): 153-161.

**Figure captions**

**Figure 1. ECG tracings for CH characteristics in experimental groups (graphical representation of ECG scaled to the raw real time recordings).** Elevated R-amplitude with prolonged R-R interval depicting delayed heart rate (HR) with mildly widened QRS complex were observed in DOX administered rats when compared to the normal.

**Figure 2. Heart morphology.** The DOX administered rats revealed enlarged heart sizes especially the ventricular region than the normal heart as shown in the figure (scaled in graph).

**Figure 3. Histopathological analysis of ventricles in NOR and DOX administered rats.** The left ventricle (LV) of DOX (figure b) displayed distorted muscle fibers (DMF), loss of connective tissue separations (LCTS) and hypertrophied nuclei (HN) along with the presence of cellular infiltrations (CIF) of inflammatory cells when compared to normal (figure a). Similarly, the right ventricles of DOX administered rats (figure d) displayed patterns as identified in LV and these changes were found to be less prominent in RV than LV.

**Figure 4. Concentration of serum metabolites and unique fingerprint metabolites in experimental groups identified using GC-MS analysis.** Besides alanine, galactose and mannose that were reduced in DOX, it is worthy to note that norvaline, norleucine, ribose, erythrose, mannonic/gluconic acid, allonic acid, succinic acid and sorbitol were found highly elevated that were observed as trace in the normal.

**Figure 5. Correlation heat map for DOX induced CH.** Correlation analysis (Pearson's) revealed strong correlation between most of the serum metabolites and with the seven metabolic responders (scores $\geq 0.7$). There were no metabolites that were correlated to QRS complex. Alanine, galactose and mannose were strongly positively correlated with HR but negatively correlated with other serum metabolites and dependent factors of this study.

ISSN: 0975-3583, 0976-2833 VOL 12, ISSUE 03, 2021

**Figure 6. Pattern hunting analysis to visualize strong and weak relationship between metabolites.** No strongly correlating metabolites were identified for QRS complex. The metabolites that were strongly associated with each of the seven dependent factors (diagnostic parameters) are indicated in green box in the figure wherein galactose was found inversely related to all other metabolites.

**Figure 7. MSEA mapping of pathways influenced by predictors.** Branched chain amino acid degradation and Ketone body metabolism were identified as highly influenced pathways due to their significance values ($P < 0.05$) as well as their enrichment ratio. These pathways were mapped as influential pathways by the five predictors during early stages (end of 2 weeks) of CH development in doxorubicin administered rats. Besides these pathways, the mitochondrial electron transport chain, carnitine synthesis, oxidation of branched chain fatty acids, Phytanic acid peroxisomal oxidation were mapped as the next highly enriched pathways. Citric acid cycle, fructose and mannose degradation, galactose metabolism form the third set of enriched pathways. Steroidogenesis, steroid biosynthesis, glutamate metabolism, arginine and proline metabolism categorize the fourth enriched set with Warburg effect and bile acid biosynthesis being the least significantly enriched pathways.

**Table captions**

**Table 1. Screening CH characteristics and ventricular function using ECG**. Values expressed as mean ± S.E of 5 samples per group (ms – millisecond; bpm – beats per minute). The percentage changes in each ECG parameters are indicated by red (increase) and blue (decrease) arrows. Group comparison: a – NOR Vs DOX. Statistical significance ($P<0.05$) indicated by *. The values of normal group indicated in this table are used in a similar concomitant study conducted in our lab along with this study.

**Table 2**. **HW/BW ratio.** It shows the mean ± S.E of 5 samples per group. Group comparison: a – NOR Vs DOX. Statistical significance ($P<0.05$) indicated by *. The values of normal group indicated in this table are used in a similar concomitant study conducted in our lab along with this study.

**Table 3. Potent serum early predictors.** It indicates the predictor metabolites (independent variable) and their respective metabolic responders (dependent variable) for DOX administered rats at the end of 2 weeks. The table displays the model fitness wherein statistical significance ($P<0.05$) indicated by *. The values of normal group indicated in this table are used in a similar concomitant study conducted in our lab along with this study.

**Figures**

**Figure 1.**

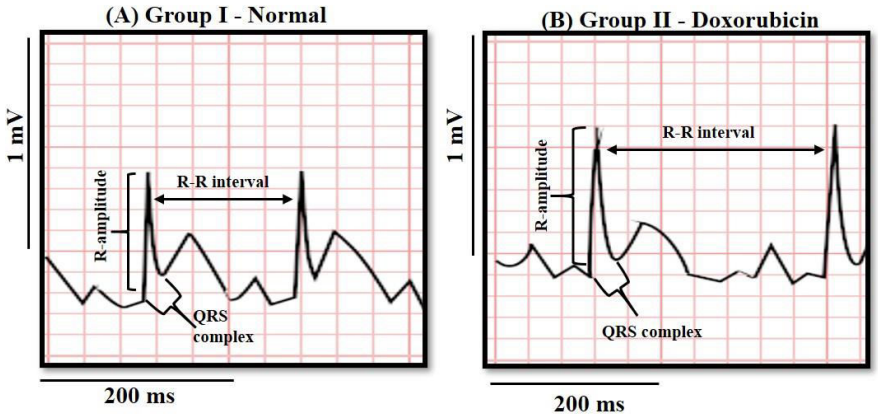

ISSN: 0975-3583, 0976-2833 VOL 12, ISSUE 03, 2021

**Figure 2.**

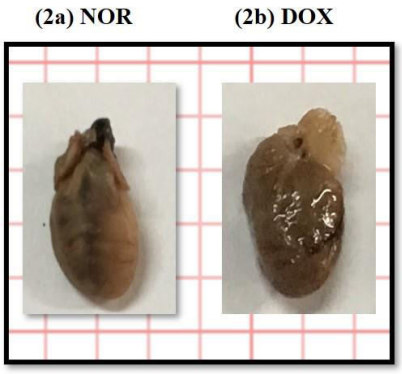


**Figure 3.**

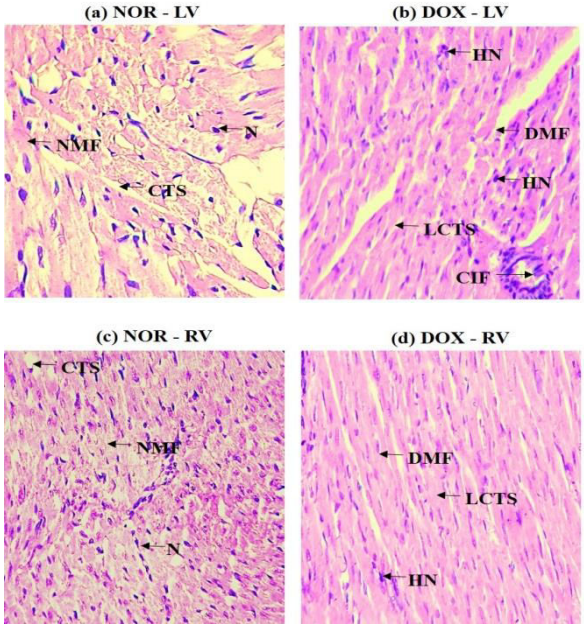


**Figure 4.**

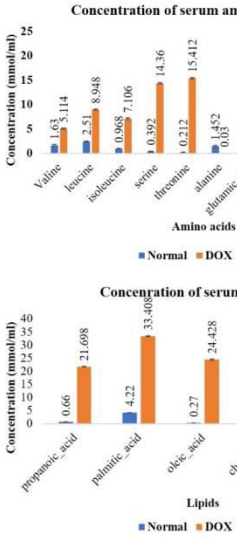

ISSN: 0975-3583, 0976-2833 VOL 12, ISSUE 03, 2021

**Figure 5**

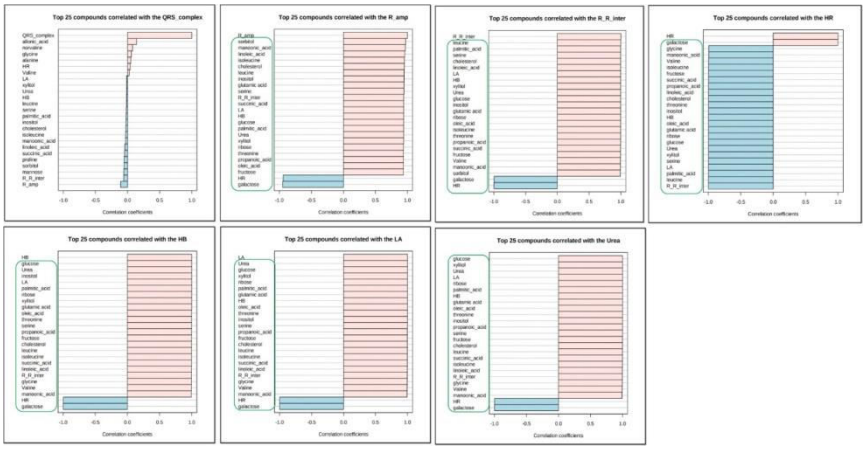


**Figure 6.**

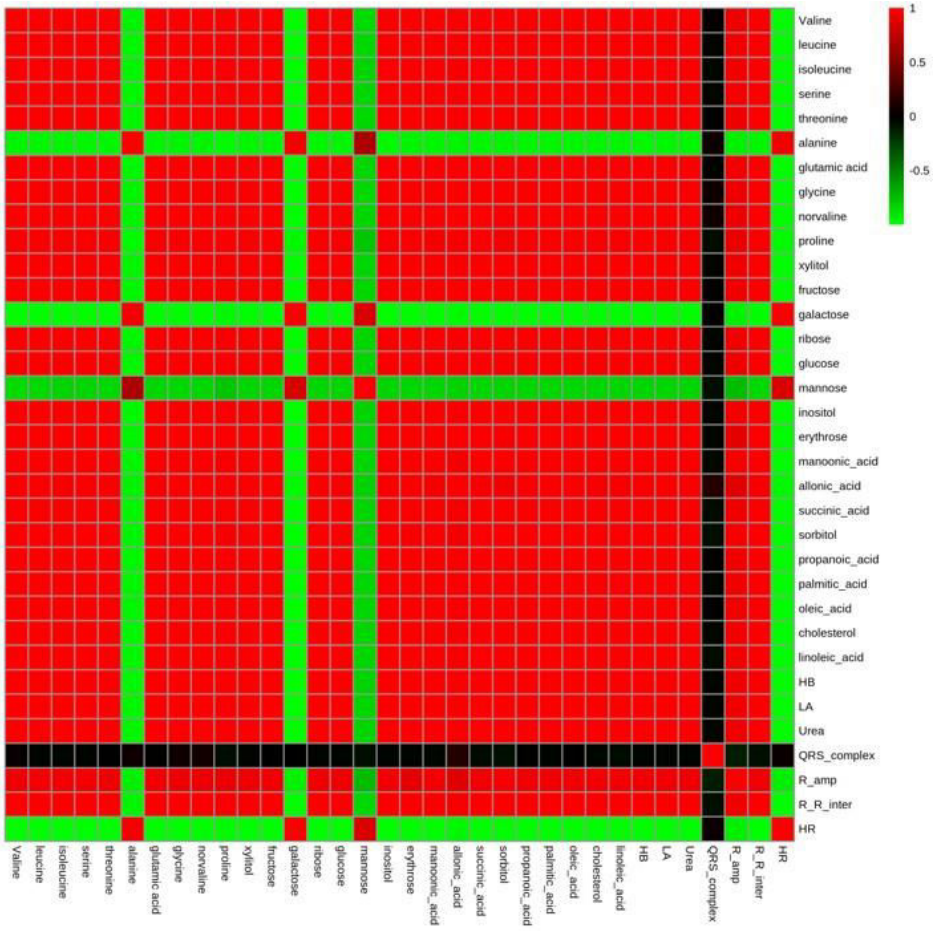

ISSN: 0975-3583, 0976-2833 VOL 12, ISSUE 03, 2021

**Figure 7.**

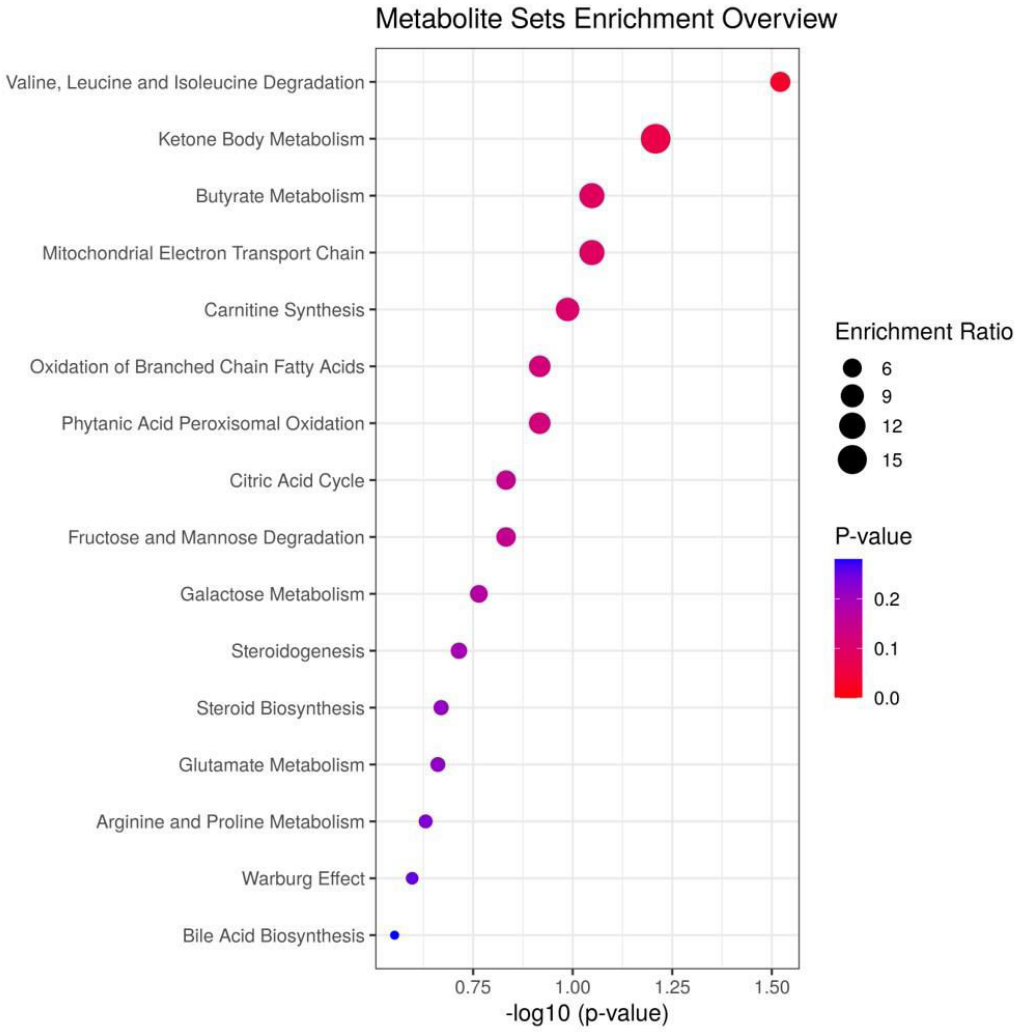


**Tables**
**Table 1**

| Metabolic responders | Potent predictor metabolite | Prediction equation | Predictor - Linear model fitness and its significance |
|---|---|---|---|
| QRS complex | - | - | - |
| R-amplitude | sorbitol | y = -1.256 + 0.620x | $R^2$=0.91; p = 0.013* |
| R-R interval | isoleucine | y = -85.680 + 38.268x | $R^2$=0.99; p = 0.00003* |
| Heart rate/Pulse rate (HR) | Mannonic acid (gluconic acid) | y = 273.721 + 52.403x | $R^2$=0.94; p = 0.0001* |
| 3-HB | cholesterol | y = -35.612 + 2.147x | $R^2$=0.99; p = 0.000001* |
| LA | Succinic acid | y = -54.716 + 8.234x | $R^2$=0.99; p = 0.000001* |
| Urea | Succinic acid | y = -167.097+ 26.445x | $R^2$=0.99; p = 0.000001* |

ISSN: 0975-3583, 0976-2833 VOL 12, ISSUE 03, 2021

**Table 2**

| Groups | QRS complex (ms) | % change | R amplitude (mV) | % change | R-R interval (ms) | % change | Heart rate (HR) (bpm) | % change |
|---|---|---|---|---|---|---|---|---|
| I - NOR | 19.30 ± 0.52 | - | 0.43 ± 0.05 | - | 162.49 ± 2.93 | - | 369.00 ± 1.77 | - |
| II - DOX | 19.40 ± 3.17[a] | 0.35 ⇧ | 0.73 ± 0.08 [a*] | 71.02 ⇧ | 280.00 ± 5.47 [a*] | 72.32 ⇧ | 214.00 ± 4.22 [a*] | 41.97 ⇩ |

**Table 3**

| Groups | Body weight (BW in g) | Heart weight (HW in g) | HW/BW ratio |
|---|---|---|---|
| I - NOR | 110.36 ± 3.65 | 0.320 ± 0.010 | 2.92 ± 0.12 |
| II - DOX | 110.00 ± 9.35[a] | 0.625 ± 0.014 [a*] | 5.71 ± 0.42 [a*] |